An *Xpd* mouse model for the combined xeroderma pigmentosum/Cockayne syndrome exhibiting both cancer predisposition and segmental progeria

Jaan-Olle Andressoo,[1,6] James R. Mitchell,[1] Jan de Wit,[1] Deborah Hoogstraten,[1] Marcel Volker,[4] Wendy Toussaint,[1] Ewoud Speksnijder,[3] Rudolph B. Beems,[3] Harry van Steeg,[3] Judith Jans,[1,5] Chris I. de Zeeuw,[2] Nicolaas G.J. Jaspers,[1] Anja Raams,[1] Alan R. Lehmann,[4] Wim Vermeulen,[1] Jan H.J. Hoeijmakers,[1,*] and Gijsbertus T.J. van der Horst[1]

[1] Medical Genetics Center, Department of Cell Biology and Genetics, Center of Biomedical Genetics, Cancer Genomics Center, Erasmus Medical Center, Dr. Molewaterplein 50, 3015 GE, Rotterdam, The Netherlands
[2] Department of Neuroscience, Post Office Box 1738, Erasmus MC, 3000DR Rotterdam, The Netherlands
[3] National Institute of Public Health and the Environment, Post Office Box 1, 3720 BA Bilthoven, The Netherlands
[4] Genome Damage and Stability Centre, University of Sussex, Falmer, Brighton BN1 9RQ, United Kingdom
[5] Present address: Department of Molecular and Cell Biology, University of California, Berkeley, 125 Koshland Hall, Berkeley, California 94720.
[6] Present address: Institute of Biotechnology, Viikinkaari 9, 00014 Helsinki, Finland.
*Correspondence: j.hoeijmakers@erasmusmc.nl

Summary

Inborn defects in nucleotide excision DNA repair (NER) can paradoxically result in elevated cancer incidence (xeroderma pigmentosum [XP]) or segmental progeria without cancer predisposition (Cockayne syndrome [CS] and trichothiodystrophy [TTD]). We report generation of a knockin mouse model for the combined disorder XPCS with a G602D-encoding mutation in the *Xpd* helicase gene. XPCS mice are the most skin cancer-prone NER model to date, and we postulate an unusual NER dysfunction that is likely responsible for this susceptibility. XPCS mice also displayed symptoms of segmental progeria, including cachexia and progressive loss of germinal epithelium. Like CS fibroblasts, XPCS and TTD fibroblasts from human and mouse showed evidence of defective repair of oxidative DNA lesions that may underlie these segmental progeroid symptoms.

Introduction

The highly conserved nucleotide excision DNA repair pathway (NER) removes a wide diversity of helix-distorting DNA lesions, including UV-induced photoproducts, bulky chemical adducts, and several forms of oxidative lesions (Brooks et al., 2000; de Laat et al., 1999; Furuta et al., 2002; Hoeijmakers, 2001; Spivak and Hanawalt, 2006). NER is composed of two subpathways, global genome NER (GG-NER) and transcription-coupled NER (TC-NER), that differ mainly in the mechanism of damage recognition. In GG-NER, the hHR23B/XPC complex, assisted for some lesions by the XPE/UV-DDB complex, functions as the main damage sensor and initiator of the NER reaction. In TC-NER, blockage of transcribing RNA-PolII is believed to trigger the repair reaction (Batty and Wood, 2000; Hanawalt, 2002; Svejstrup, 2003; van den Boom et al., 2002). NER involves sequential binding of ~30 proteins in a "cut and patch"-type reaction that takes ~4 min to complete (de Laat et al., 1999; Hoogstraten et al., 2002).

The consequences of inborn defects in NER are highlighted by rare, autosomal recessive syndromes xeroderma pigmentosum (XP), Cockayne syndrome (CS), and trichothiodystrophy (TTD) (Bootsma et al., 2002; Broughton et al., 2001; Lehmann, 2003). XP patients display prominent sun sensitivity, elevated (>1000-fold) frequency of sun-induced skin cancer, and >10-fold risk of internal tumors (Kraemer et al., 1987). Enigmatically, the sun sensitivity in CS and TTD does not result in enhanced cancer risk. Instead, these syndromes are characterized by postnatal developmental delay, microcephaly, skeletal abnormalities, progressive mental degeneration, sensorineural deafness, ataxia, spasticity and gait anomalies, demyelination, brain calcifications, hypogonadism, and death usually before puberty

SIGNIFICANCE

The notion that defects in NER give rise to either segmental progeria (CS and TTD) or cancer predisposition (XP) led to the hypothesis that premature aging can protect against cancer, likely via activation of cell death or senescence pathways following genotoxic insult. However, the rare combined cases of XPCS and XPTTD in which both cancer and progeria coemerge present a challenge to this notion. Using a mouse model for XPCS, we show that cancer and segmental progeria can be differentially modulated by one amino acid substitution in a single protein, the XPD helicase component of the transcription/repair factor TFIIH.

(Itin et al., 2001; Nakura et al., 2000; Nance and Berry, 1992; Rapin et al., 2000). In addition to these features reminiscent of premature aging, TTD patients display typical brittle hair and nails and scaling skin (ichthyosis). However, in exceptional cases, NER deficiency presents as a combined syndrome, XPCS (Lafforet and Dupuy, 1978) or XPTTD (Broughton et al., 2001), in which the hallmarks of both XP and CS or TTD coexist. Because these disorders are so rare (only nine XPCS and two XPTTD patients reported) and clinically heterogeneous, firm conclusions about the relationship between cancer and aging in NER disorders have so far been elusive.

While enhanced mutagenesis is accepted as the mechanistic basis of elevated skin cancer incidence in XP (Cleaver, 2000; Hoeijmakers, 2001; Lehmann, 2005), the molecular deficiency underlying segmental progeria remains obscure as well as the relationship between cancer and aging (Mitchell et al., 2003). Mutations in genes encoding three of the ten components of the multifunctional protein complex TFIIH—XPB, XPD, and p8/TTD-A—are associated with the widest clinical diversity, ranging from XP to XPCS, TTD, and XPTTD (Broughton et al., 1994, 2001; Giglia-Mari et al., 2004; Weeda et al., 1997). In DNA repair via the NER pathway, the XPB and XPD helicase subunits of TFIIH, together with p8/TTD-A, cooperate to unwind DNA surrounding the lesion (Coin et al., 2006). TFIIH also opens promoters for RNA polymerase (Pol)II (Schaeffer et al., 1993), and RNA PolI transcription (Bradsher et al., 2002; Hoogstraten et al., 2002) and mediates some forms of activated transcription (Keriel et al., 2002). In addition, TFIIH has putative roles in p53-dependent apoptosis (Wang et al., 1996), cell cycle regulation (Harper and Elledge, 1998), and resistance to oxidative stress (de Boer et al., 2002; de Waard et al., 2003, 2004). To what extent any of these defects, whether in DNA repair, transcription, or cell cycle control, contribute to disease etiology in vivo is still largely unknown, mostly due to limitations of existing biochemical and cellular assays to predict systemic and/or time-dependent pathology.

The aim of this study was to investigate the mechanism(s) of TFIIH-associated segmental progeria and cancer predisposition in experimentally tractable mouse models of the XPD-associated progeroid disorders TTD and XPCS. Previously, we mimicked a known human TTD-associated point mutation (XPD^{R722W}) in the mouse *Xpd* locus. Homozygous Xpd^{TTD} mice constitute an excellent model for human TTD displaying the hallmark cutaneous symptoms as well as segmental progeroid features (de Boer et al., 1998a, 2002). Further reduction of DNA repair capacity by inactivation of the *Xpa* gene results in acceleration of TTD features and death within 3 weeks after birth (de Boer et al., 2002). Here, we report the generation and characterization of an Xpd^{XPCS} mouse model engineered by genocopying the XPD^{G602D} allele found in the patient XPCS2.

Results

Generation of viable Xpd^{XPCS} knockin mice

Because the XPD protein is essential for viability (de Boer et al., 1998b) and previous attempts to mimic the XPD^{XPCS} (Xpd^{G602D}) point mutation failed to yield a viable mouse mutant (J.-O.A., unpublished data), we adopted a minimally invasive knockin strategy as depicted in Figures 1A–1C. Briefly, the *Xpd* locus was targeted by homologous recombination in ES cells with the G602D-encoding point mutation together with a loxP-flanked neomycin resistance cassette in the 3′UTR. Progeny of chimeric mice generated with the targeted ES cells heterozygous for the XPCS-neo-LoxP G602D *Xpd* allele (Figures 1B and 1D) were subsequently crossed with Cre recombinase-expressing mice to generate the XPCS allele (Figures 1C and 1E). RT-PCR from testes RNA of heterozygous animals demonstrated comparable mRNA expression between wt and mutant alleles (Figure 1F).

$Xpd^{XPCS/XPCS}$ homozygous mutant offspring from matings between heterozygous animals were viable and observed at the expected Mendelian frequency. Despite similar Xpd mRNA levels, TFIIH levels were significantly reduced to ~50% of wt in primary XPCS mouse embryonic fibroblasts (MEFs; Figures 1G and 1H). Reduced TFIIH was also observed in cells from patient XPCS2 (Botta et al., 2002). Because $Xpd^{wt/wt}$ and heterozygous $Xpd^{XPCS/wt}$ mice were indistinguishable in all aspects investigated, we conclude that the mutant allele has no dominant effect over the wild-type allele, consistent with the recessive nature of the disease. For simplicity, $Xpd^{wt/wt}$ and $Xpd^{XPCS/wt}$ mice will hereafter be referred to as "wt" and homozygous mutants as "XPCS." Unless noted otherwise, all the mice used in this study were in a 129Ola/C57BL/6/FVB hybrid genetic background.

Repair of UV-induced damage in XPCS cells

Fibroblasts from the XPCS patient XPCS2, a hemizygote with XPD^{G602D} expression from one allele, display defects in both GG-NER and TC-NER and are hypersensitive to killing by UV (Broughton et al., 1995). We tested various DNA repair characteristics of primary MEFs using the UV-induced *u*nscheduled *D*NA *s*ynthesis (UDS) and *r*ecovery of *R*NA *s*ynthesis (RRS) assays, which reflect GG-NER and TC-NER activities, respectively. Similar to XPA and CSB cells, which lack TC-NER capacity entirely, XPCS cells had no detectable RRS (Figure 2B). However, unlike XPA cells, which lack GG-NER altogether, XPCS cells retained ~30% UDS activity (Figure 2A). Consistent with a NER defect and similar to cells from patient XPCS2, primary XPCS MEFs were hypersensitive to UV irradiation (Figure 2C).

We next examined the kinetics of NER factor accumulation at locally induced UV damage in the nuclei of wt and mutant cells. The accumulation and retention of NER factors at sites of local damage mainly reflects GG-NER of UV-induced 6-4 photoproducts, a process which is completed in ~2 hr in wt cells (D.H., unpublished data). We monitored Xpc, the main damage sensor in GG-NER, and the p62 subunit of TFIIH by immunofluorescence 15 min and 3 hr after application of local UV damage. In XPA and XPCS MEFs, we consistently observed accumulation of both XPC and TFIIH at sites of UV irradiation within 15 min of UV exposure at concentrations similar to those observed in wt MEFs. Three hours after UV, when NER factors were no longer detectable at local damage in wt cells, XPC and TFIIH remained concentrated at local damage in XPA, in XPCS, and to a lesser extent in partially NER-defective TTD MEFs (Figure 2D and data not shown). Interestingly, in double mutant XPA|XPCS cells, XPC displayed normal accumulation, whereas TFIIH binding at local damage was either weak (~50% of cells) or below the level of detection (~50% of cells) (Figure 2D). Similar results were obtained in double mutant XPA|TTD cells (data not shown), indicating that the absence of XPA reduces binding of TFIIH to damage when carrying XPCS (XPD^{G602D}) or TTD (XPD^{R722W}) alterations.

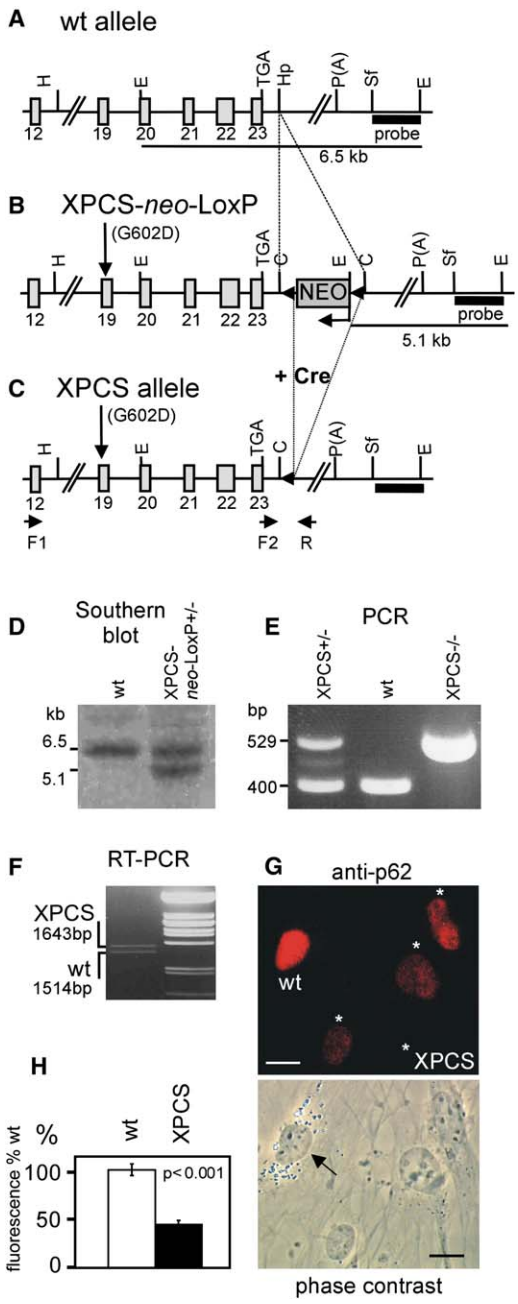

Figure 1. XPCS knockin targeting of the mouse *Xpd* locus

A–C: Schematic representation of the wild-type (**A**), targeted (**B**), and Cre recombined (**C**) *Xpd* loci. Coding exons are numbered. Causative G602D mutation is indicated by a vertical arrow and LoxP sequences by filled triangles. Primers F1, F2, and R are indicated by arrows. TGA, translational stop codon; P(A), polyadenylation signal. H, HindIII; E, EcoRI; Hp, HpaI; Sf, SfiI.

D: Southern blot of EcoRI-digested genomic DNA from wt and XPCS-*neo*-LoxP recombinant ES clones hybridized with a unique 3′ probe located outside the targeting construct (**A**–**C**, thick line). wt allele, 6.5 kb; targeted allele, 5.1 kb.

E: Verification of Cre excision of the *neo* gene and genotyping of progeny by PCR using primers F2 and R as indicated in **C**. After excision by Cre, the XPCS and wt alleles yield products of 529 and 400 bp, respectively.

F: RT-PCR amplification of mRNA originating from $Xpd^{XPCS/wt}$ testis using primers R and F1. Note the comparable amounts of 1514 bp wt and 1643 bp XPCS products.

G: Upper panel: indirect immunofluorescence of the p62 subunit of TFIIH in wt and XPCS primary MEFs (indicated by asterisks). Lower panel: phase contrast image of the same microscopic field; wt cell is labeled with silicon beads (arrow). Scale bars, 5 μm.

H: Quantification of immunofluorescence from the p62 subunit of the TFIIH complex in wt and XPCS cells. p value indicates the significance of the difference between wt and XPCS cells analyzed on the same microscopic slide. Error bars indicate SEM.

Hypersensitivity to UV irradiation in XPCS mice

Photosensitivity is a common symptom of NER deficiency independent of skin cancer predisposition. In contrast to wt controls, XPCS mice exposed to UV-B light at the environmentally relevant dose of 200 J/m^2/day for 4 days developed erythema within 5 days (data not shown). Histological analysis of skin sections of XPCS mice sacrificed 1 week after the start of UV-B treatment revealed pronounced epidermal hyperplasia, consisting of an increased number of viable cell layers (acanthosis) and hyperemia (dilated capillaries, filled with blood), reflecting the observed skin erythema (Figure 3A). Neither erythema nor hyperplasia was observed in the UV-exposed skin of heterozygous mice and in the unexposed skin of XPCS mice (Figure 3A). In conclusion, the XPCS mutation induces severe photosensitivity in mice similar to that of patient XPCS2.

Enhanced cancer predisposition and a unique repair defect in XPCS mice

The XPCS patient XPCS2 first presented with a skin tumor already at 2.5 years of age (Lafforet and Dupuy, 1978; Lindenbaum et al., 2001), suggestive of a pronounced cancer predisposition. In order to determine skin cancer susceptibility, we exposed XPCS animals daily to a low UV-B dose of 100 J/m^2/day (equivalent to ~70% of the minimal erythemal dose for XPCS, ~50% for XPA, ~10% for wt). NER-deficient XPA mice in a C57BL/6 genetic background were included as a positive control. Four out of ten XPCS mice and zero out of five XPA mice developed corneal opacity 10 weeks after the start of the UV-B treatment; at 11 weeks, all ten XPCS mice and three out of five XPA mice showed corneal opacity. Cutaneous effects (i.e., erythema) were observed in UV-treated XPCS but not XPA mice at 7 weeks after the start of the treatment (three out of ten mice). Within 17 weeks, all ten XPCS mice developed skin and/or eye tumors on UV-B exposed areas (Figures 3B–3D; Table 1), whereas none of the XPA mice carried tumors at this time point. At 23 weeks, the first tumor-bearing XPA mouse was observed, with all five XPA mice carrying tumors by 31 weeks. During the 40 week experiment, none of the wild-type or heterozygous control mice developed tumors or other skin lesions. A complete overview of the observed tumor response is given in Table 1. A summary of published UVB carcinogenesis experiments in NER mouse models is presented in Table S1 in the Supplemental Data available with this article online.

The uniform, rapid onset of tumors in XPCS mice and the absence of clear strain-associated changes in cancer predisposition in XPA (Table S1) and TTD mice (exposure of TTD mice in C57/bl6 background to a daily dose of 80 J/m^2 revealed no cancer predisposition; J.J. and H. Rebel, unpublished data) indicates that the XPD^{G602D}-encoding mutation, rather than the genetic background, is causative of the cancer predisposition. Thus, among NER-deficient mice, XPCS appears the most prone to UV-induced skin cancer.

We next explored why XPCS mice are more cancer prone than XPA mice, which lack the ability to repair UV-induced DNA lesions by NER altogether. In wt cells, the "cut" (incision)

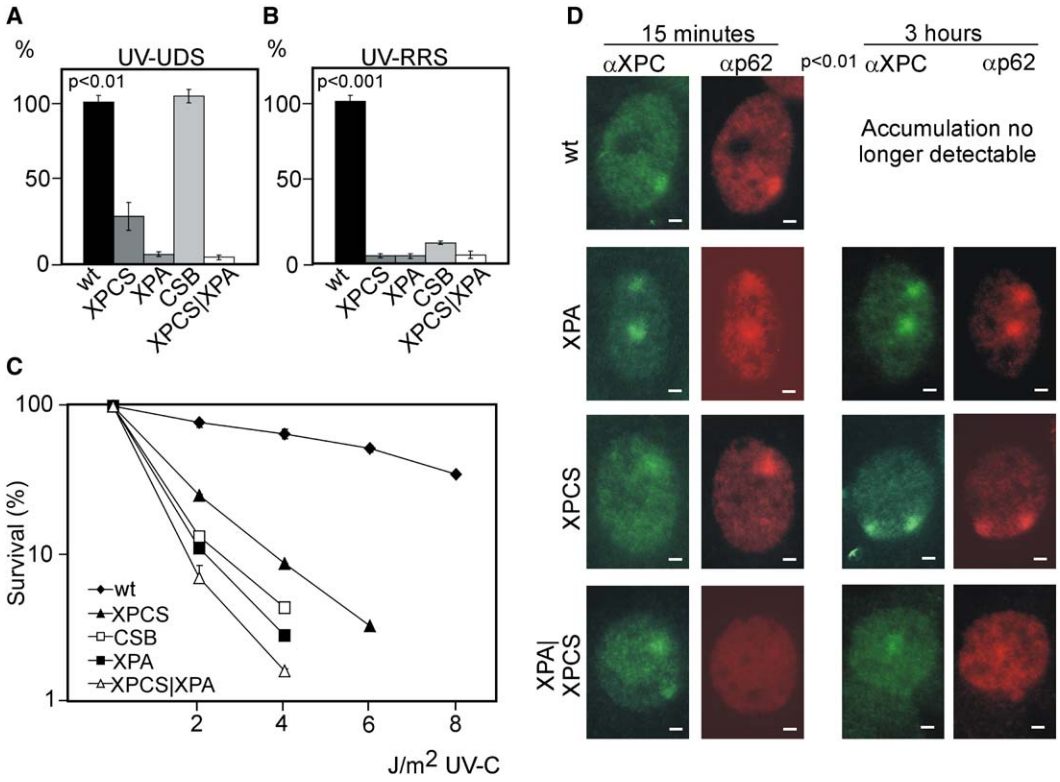

Figure 2. UV-induced DNA damage repair characteristics of XPCS cells

A: UV-induced DNA repair synthesis capacity (UV-UDS) in primary MEFs of the indicated genotypes. p value indicates the significance of the difference between wt and CSB to XPCS, XPA, and XPCS|XPA as well as between XPCS and XPA mutants. Error bars indicate SEM.

B: UV-induced recovery of RNA synthesis (UV-RRS) in primary MEFs. p value indicates the significance of the difference between all of the mutants and the wt. Error bars indicate SEM.

C: Composite UV survival from several independent experiments containing multiple primary MEF lines per genotype. Error bars lie within symbol size and indicate SEM between different experiments.

D: Kinetics of UV-induced NER factor accumulation. XPC and the p62 subunit of TFIIH were visualized by indirect immunofluorescence at 15 min and 3 hr after local UV irradiation of primary MEFs of the indicated genotypes. Note the lack of observable TFIIH accumulation at UV-irradiated sites in nuclei of cells doubly mutant for XPA and XPCS. Scale bars, 1 μm.

and "patch" steps of NER-dependent DNA repair synthesis (as measured by UDS) are coupled to each other as well as to lesion removal, while in UV-irradiated XPCS patient-derived cells, incision activity is high despite relatively low UDS and virtually absent lesion removal (Berneburg et al., 2000; Theron et al., 2005), indicating an uncoupling of these repair parameters. To determine if this uncoupling is also present in cells from the XPCS mouse model, we followed the phosphorylated histone H2AX (γH2AX) as a marker of incision activity 3 hr after UV treatment of nondividing wt, XPCS, and TTD primary MEFs. UV-induced γH2AX formation in nondividing cells reflects at least in part NER incision activity and is reduced in XPA-deficient human (O'Driscoll et al., 2003) and mouse cells (Theron et al., 2005). γH2AX staining in XPCS cells was greater than that in wt cells upon UV treatment (Figure 3E), indicative of an increased number of incisions despite reduced UDS. In TTD cells as in XPA cells, reduced UDS activity was paralleled by a reduction in γH2AX staining (Figure 3E). Thus, elevated levels of UV-induced incisions uncoupled from repair synthesis (UDS) are a property of XPCS but not TTD cells in both man and mouse.

Low UDS relative to wt may still suggest UV lesion removal but at a reduced rate. We thus tested the kinetics of lesion removal at locally UV-irradiated regions of the nucleus in human cell lines including representative XPD^{XPCS}, XPD^{XP}, XPD^{TTD}, wt, and TTD cells defective in another TFIIH subunit, p8/TTD-A. UV-induced DNA lesions were visualized directly using antibodies against 6-4 photoproducts or indirectly by the accumulation of NER factors XPC and TFIIH (Table 2 and data not shown). Consistent with earlier biochemical findings (van Hoffen et al., 1999), lesions remained in XPD^{XP} and XPD^{XPCS} cells up to 8 hr following UV treatment despite residual UDS levels ~30%–40% of wt. In TTD cells with 15%–50% residual UDS, however, lesions were largely removed within 8 hr after UV. Thus, unlike in wt and TTD cells, the low levels of repair synthesis (UDS) observed in XPD^{XP} and XPD^{XPCS} cells do not represent actual lesion removal. We now refer to this futile NER-related DNA synthesis activity as "phantom" UDS. Taken together, these data suggest that the unique UV-induced skin cancer predisposition observed in XPCS mice may be caused by a combination of common and unique NER defects: namely, the failure to remove UV lesions, a property shared with XPA deficiency, and uncoupled cut and patch mechanisms resulting in both γH2AX foci and phantom UDS, a property unique to XPCS.

CS-specific developmental and progeroid features in XPCS mice

Developmental delay in CS-affected humans has an almost exclusive postnatal onset (Nance and Berry, 1992). Although born

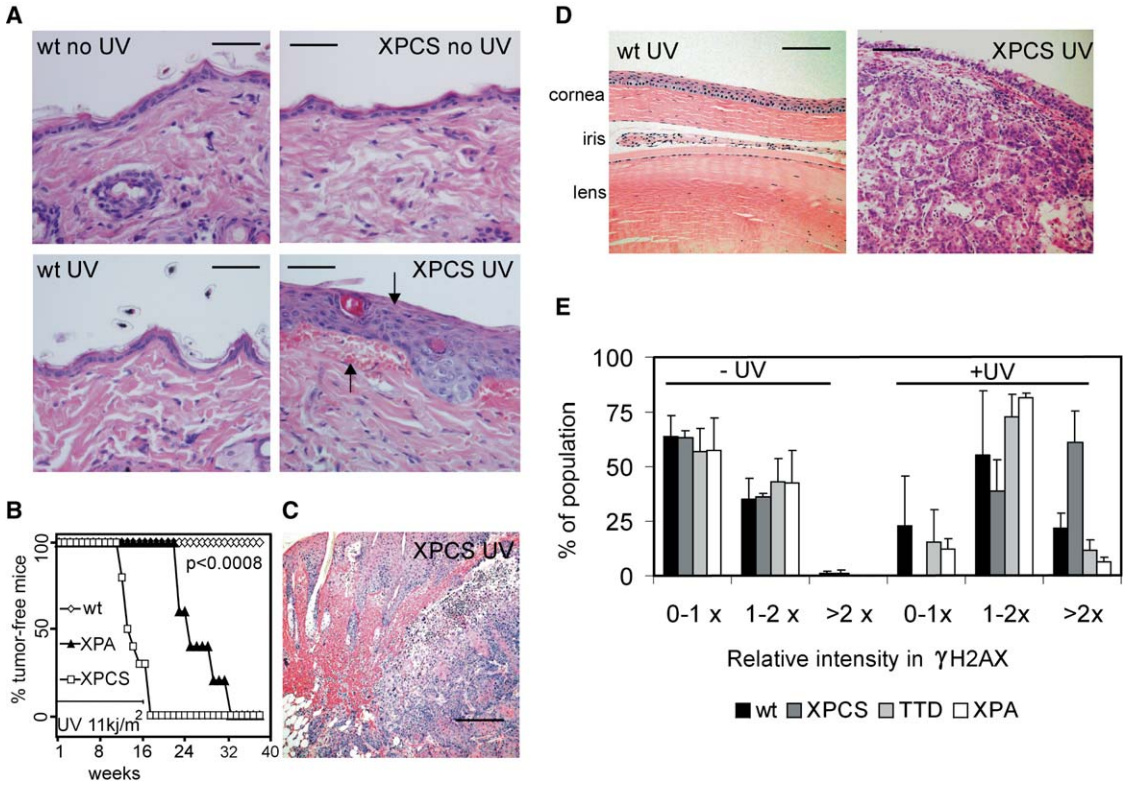

Figure 3. Acute and chronic effects of UV-B on XPCS mice

A: Skin sections of the indicated genotypes following acute UV-B exposure. Note the pronounced epidermal hyperplasia (increased number of viable cell layers; arrow above), hyperemia (dilated capillaries filled with blood; arrow below), and absence of a keratinized layer reflected by ''scaling of the skin'' at the macroscopic level. H&E; scale bars, 20 μm.

B: Time course of tumor formation in XPCS and XPA mice during chronic UV-B exposure.

C: Example of a typical squamous cell carcinoma invading subcutaneous tissues from a UV-B exposed XPCS mouse. H&E; scale bar, 160 μm.

D: UV-B-irradiated cornea of wt and XPCS mice as indicated. Note the squamous cell carcinoma in the eye of an XPCS mouse. H&E; scale bars, 80 μm.

E: Quantification of γH2AX immunofluorescence indicative of DNA breaks in nuclei before (−) and 3 hr after (+) UV irradiation in primary wt, XPCS, TTD, and XPA MEFs. 1× relative intensity represents the average amount of γH2AX immunofluorescence in the corresponding unirradiated cell line; cells with >2× this amount were considered γH2AX positive. Error bars indicate SD.

at the expected Mendelian frequencies and with normal birth weights, XPCS mice displayed a small but significant developmental delay present at about 5 days after birth and persisting at least until 16 days for both male and female XPCS pups (Figure 4A). While female XPCS mice caught up with littermate controls between ~2 and 4 weeks of age, the developmental delay in male XPCS mice lasted until about 2 months of age (Figures 4B and 4C), during which tail suspension tests of male but not female XPCS mice occasionally revealed spastic and abnormal coordination of hindlimbs (Figure 4D). No correlation between the extent of developmental delay and neurological features was observed. After 2 months, the neurological features became less pronounced and gradually disappeared among most, but not all, of the 20 male XPCS animals examined.

Gross behavior, cognitive ability, and neuromotor function of XPCS mice were analyzed by behavioral tests. Although male XPCS mice showed normal behavior, they were significantly less active within the first minute of an open-field exploratory test ($n = 12$ and 17 for XPCS and wt animals, respectively; $p < 0.03$), indicating that XPCS mice require longer adaptation

Table 1. UV-induced tumorigenesis in XPCS mice

		Tumor	Incidence	
Genotype	wt or hz	XPCS	XPA	Tumor types found (× incidence)
UV-treated (at 17 weeks after start of UV)	0/7	10/10*, average latency 13 weeks	0/5	SCC of an eye, 4× (cases); 8× SCC + 2 SCP of the skin; hemangioma of an eye, 2×
UV-treated (at 31 weeks after start of UV)	0/7 (also at 41 weeks)	—	5/5*, average latency 25 weeks	SCC of an eye, 1×; 6× SCC + 1× SCP of the skin

hz, XPCS heterozygous; SCC, squamous cell carcinoma; SCP, squamous cell papilloma. *Significant difference in average tumor latency time for XPCS mice versus XPA mice, $p < 0.0008$.

Table 2. UDS and kinetics of damage removal in human XP, XPCS, and TTD cells

Cell line	UDS, percent of the wt	Relative XPC intensity at local UV damage	
		15 min	8 hr
C5RO (wt)	100%	+++	—
XP6BE (*XPD*^{XP})	~40%[d]	+++	+++
XP1NE (*XPD*^{XPCS})	~40%[a]	+++	+++
XPCS2 (*XPD*^{XPCS})	~30%[b]	+++	++
TTD1BEL (*XPD*^{TTD})	~15%[c]	+++	—
TTD1RO (*XPD*^{TTD})	~50%[d]	+++	—
TTD1BR (*p8*^{TTD})	~25%[e]	+++	—

Note that UDS in wt (C5RO) is set at 100%. + indicates relative intensity of immunostaining signal of XPC (immunostaining of the p62 subunit of TFIIH and 6-4 photoproducts yielded similar results; data not shown).
[a]Taylor et al. (1997).
[b]Takayama et al. (1995).
[c]Broughton et al. (1994).
[d]Takayama et al. (1996).
[e]Stefanini et al. (1993).

time in a new environment. No age-specific differences were found up to 7 months of age, suggesting that within this age range this feature has no progressive character (data not shown). Next, neuromotor coordination and learning capacity were examined with the accelerating rotarod test. XPCS mice (n = 22) appeared normal. Footprint pattern analysis did not reveal any gait abnormalities (data not shown). Both male and female XPCS mice were fertile until at least 6 months of age and produced litters of normal size (data not shown). However, longitudinal histological analysis revealed progressive loss of germinal epithelium in the testis (Figure 4F). Cerebellum, in which loss of Purkinje neurons is believed to contribute to ataxia in CS patients, appeared unaffected in XPCS mice up to 19 months of age as concluded from immunohistochemical analysis of Purkinje neurons using calbindin antibody staining (data not shown).

We next addressed progeroid aspects related to the XPCS mutation in a life span study with 45 wt and 46 XPCS animals. Early cachexia (loss of subcutaneous fat tissue) is a common segmental progeroid feature both in CS patients (Nance and Berry, 1992) and in a mild form in CSB mice (H.v.S., unpublished data). At 6 months of age, no significant difference in body weight between wt and XPCS animals was noted. From 12 months onward, female XPCS mice displayed reduced body weight (Figure 4C). Cachexia was also observed in three out of four male XPCS animals that survived to 20 months of age, with weights of 21, 28, 31, and 41 g, while none of the 18 control animals were below 34 g (average 41 g; SE = 1 g) at that age.

The mean life span of XPCS mice (546 days; SE = 22.7) versus control mice (641 days; SE = 43.3) was significantly reduced (log rank $p = 0.001$). Animals judged to be in poor overall condition and/or animals with obvious internal or external tumors were sacrificed and autopsied. Although the percentage of mice with tumors at the end of their lives was similar (73% in wt versus 80% in XPCS), the average life span of animals bearing tumors at the time of sacrifice or autopsy was 584 ± 24.7 days in XPCS versus 744 ± 39.2 days in wt animals ($p < 0.002$), suggesting an earlier onset of spontaneous tumors in XPCS animals. Tumors were observed in liver, lung, ovary, kidney, and lymph node of wt animals, and in the liver, lungs, ovaries and testis, eye, and lymph node in addition to three papillomas of the skin in XPCS mice.

CS and sensitivity to oxidative DNA damage

Although oxidative DNA damage has long been suspected in the etiology of NER-related segmental progerias, solid supporting data have been few (Cozzarelli, 2003). Cells deficient in TC-NER due to CSB mutations (human and mouse) are hypersensitive to acute oxidative stress such as that induced by gamma irradiation or paraquat (de Waard et al., 2003, 2004; Spivak and Hanawalt, 2006). We observed hypersensitivity of spontaneously transformed XPCS MEFs to γ irradiation (Figure 5A) consistent with a CS-type defect in the repair of oxidative DNA damage.

Recently, SV40-immortalized CSA or CSB fibroblasts were also shown to be defective in their ability to express a reporter gene from a plasmid containing specific oxidative lesions upon transient transfection (Spivak and Hanawalt, 2006). Because survival/proliferation assays are influenced by many factors in addition to DNA repair capacity, we further optimized this host cell reactivation assay in order to more directly test the ability of NER-deficient cells to repair oxidative DNA lesions. We employed a dual firefly/renilla luciferase readout with a damaged renilla luciferase-encoding plasmid and an undamaged firefly luciferase-encoding plasmid in order to better control for transfection efficiency.

Ionizing irradiation was used to induce a spectrum of mainly oxidative-type lesions for transfection into spontaneously immortalized MEFs or SV40-immortalized human fibroblasts. Both murine and human CS, TTD, and XPCS cells were less proficient at reactivating the luciferase-encoding plasmid than wt (Figures 5B and 5C). Although small, differences were reproducible and significant. As a control, the ability of CS, TTD, and XPCS cells to reactivate UV-irradiated plasmid correlated positively with the UV sensitivity of the corresponding genotypes, with TTD cells closest to wt reactivation, CSB intermediate, and XPCS least able to reactivate (Figures 5B and 5C, insets).

To determine if specific types of oxidative lesions within the spectrum of ionizing radiation damage contributed to the differential reactivation capacity of NER mutants, we induced 8-oxoG and thymine glycols in the reporter plasmid using OsO_4 and methylene blue with light, respectively. For each type of damage in both human and mouse cells, wt cells were better able to reactivate the reporter plasmid (Figures 5B and 5C, insets). However, due to small magnitudes and considerable interassay variability, these differences reached statistical significance only in XPCS for 8-oxoG (human) and TTD for thymine glycol (human and mouse). We conclude that multiple types of oxidative damage are likely to contribute to the reactivation deficiency observed in these NER mutant cells.

Xpa ablation induces a similar phenotype in both XPCS and TTD models

Previously, we found that further reduction of DNA repair capacity in TTD mice by concomitant inactivation of *Xpa* severely exacerbates TTD features. XPA|TTD double mutant mice are born normally but display enhanced progressive postnatal growth failure, disproportionally big head and limbs, kyphosis, ataxia, spasticity, balance problems, gait anomalies, severe cachexia, and death around 2–3 weeks of age (de Boer et al., 2002). XPA|XPCS double mutant mice were born normally, ruling out

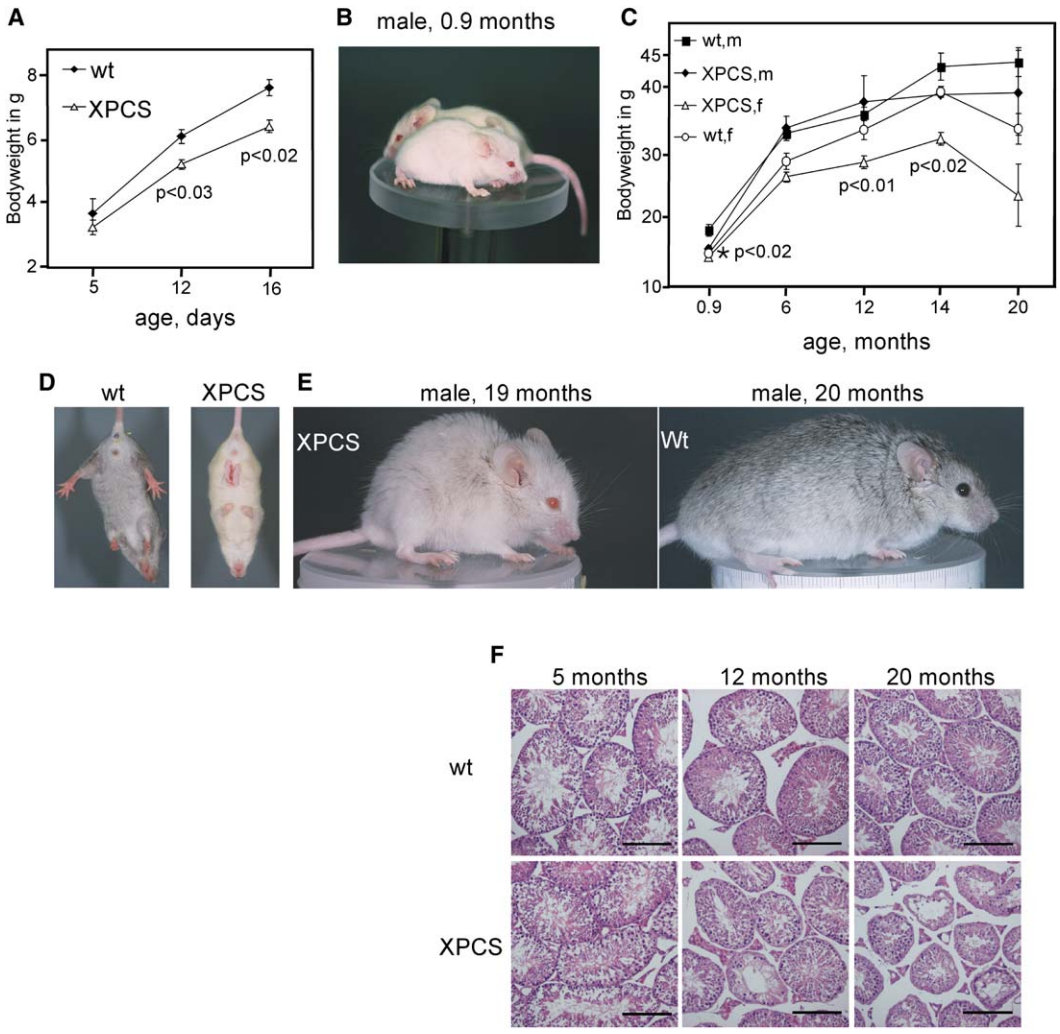

Figure 4. Phenotype of XPCS mice

A–C: Developmental delay in XPCS mice. Body weight of three independent groups of XPCS mice were measured at 5, 12, and 16 days (**A**) and from 0.9 (45 wt + 46 XPCS) to 20 months (**C**). Error bars indicate SEM. Note the smaller size of the male XPCS mouse (in front) compared to a littermate control at 0.9 months (**B**).
D: Tail suspension test of 6-week-old male mice. wt behavior includes spreading of hindlimbs and active movements with forelimbs. XPCS mice displayed heterogeneous phenotype including abnormal clasping of hind- and forelimbs (depicted), occasional tremors, and complete inactivity upon tail suspension.
E: Accelerated appearance of cachexia and kyphosis in male XPCS mice at 19 months of age compared to an age-matched wt control.
F: Progressive loss of germinal epithelium in the testis of male XPCS mice. H&E; scale bars, 80 μm.

impaired embryonal development (Figure 6B), and displayed symptoms similar to XPA|TTD mice (Figures 6A and 6C and data not shown). Growth failure in XPA|XPCS mice was not due to impaired nursing, as double mutant mice were lactated normally by the mother based on the presence of milk in the stomach of the pups analyzed at 8–12 hr and 5, 12, and 20 days after birth (data not shown). Analogous to XPA|TTD mice, life span could not be extended by providing newly lactating mothers at the age of ~20 days. Observational and footprint analyses of XPA|XPCS mice revealed progressive disturbed balance, ataxia, gait abnormalities, tremors, and spasticity during ongoing movements, suggesting that neurodysfunction in XPA|XPCS and XPA|TTD double mutant mice is similarly dramatically more pronounced than that in either of the single mutant TTD or XPCS animals. Neuropathological analyses of XPA|XPCS mice using a variety of stainings (i.e., acetylcholine esterase, silver and Nissle stainings, as well as immunohistochemical detection of calbindin, dopamine, and tyroxine hydroxylase) revealed a loss of Purkinje cells at the age of 20 days (Figure 6D). This included loss of both proximal and distal dendrites as well as cell bodies and is indicative of a degenerative process. The morphology of the remaining Purkinje cells at 20 days of age looked relatively normal with a characteristic two-dimensional dendritic tree reaching the top of the molecular layer; calbindin staining indicated an average reduction of Purkinje cells to 69% (± 18%) in the vermis and 31% (± 14%) in the hemispheres. The silver-stained sections of day 20 XPA|XPCS mice did not reveal any prominent evidence for secondary degeneration in the granule cell layer or inferior olive. This suggests that the maximal age period of ~3 weeks is insufficient to allow such a degenerative process to progress beyond the loss of Purkinje neurons. In addition, we did not observe any degeneration in higher brain regions such as the striatum, hippocampus, cerebral cortex, or thalamus as reported for several

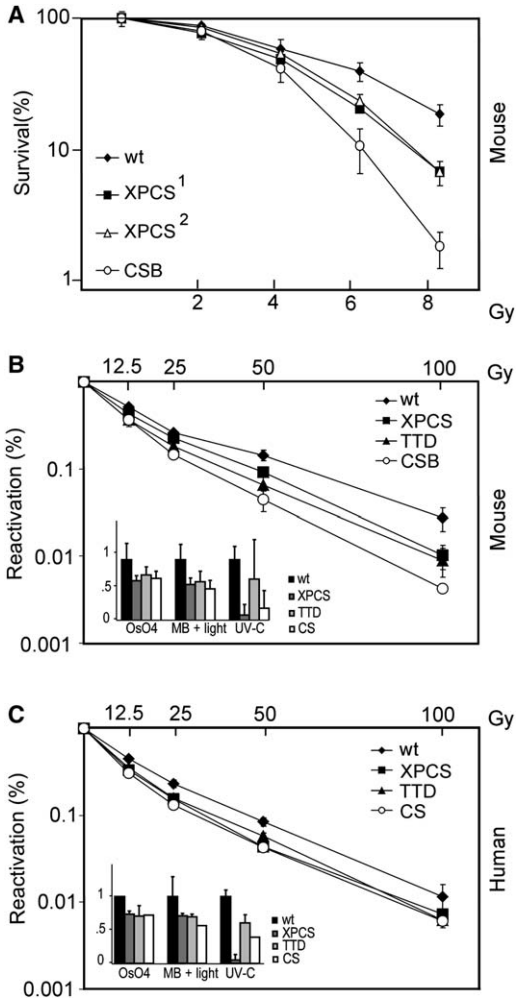

Figure 5. Oxidative DNA damage repair characteristics of XPCS cells

A: Representative ionizing radiation survival curve of two independent spontaneously immortalized XPCS MEF lines (indicated by the numbers). Error bars indicate SEM within the experiment.

B and C: Host cell reactivation in spontaneously immortalized MEFs (**B**) and SV40-transformed patient cells (**C**) of the indicated genotypes. Luciferase-encoding plasmid DNA was treated with ionizing radiation of the indicated dose (gy) or with OsO4 to generate thymine glycols, methylene blue with light to generate 8oxoG, or 400 J/m^2 UV-C (insets) as indicated. Error bars indicate SEM between three and four independent experiments. Differences between wt and XPCS and TTD (mouse and human) or CSB (mouse) were statistically significant ($p < 0.05$) at at least two doses of ionizing radiation.

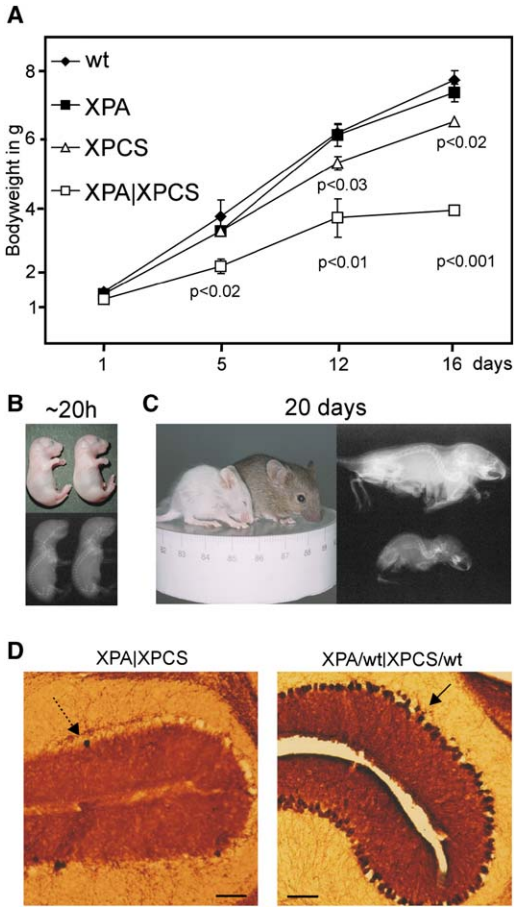

Figure 6. XPA ablation exacerbates segmental progeroid features of XPCS mice

A: Body weights of four independent cohorts of mice measured at ~20 hr after birth and at 5, 12, and 16 days of age. Error bars indicate SEM.

B and C: Light and X-ray photographs of XPA|XPCS (left) and littermate control (right) mice ~20 hr (**B**) and 20 days (**C**) after birth demonstrate the postnatal and progressive nature of cachexia and reduced bone mineral density in XPA|XPCS mice.

D: Loss of Purkinje cells in the cerebellum of XPA|XPCS mouse but not in littermate control at the age of 20 days. Arrows indicate Purkinje cell bodies. Calbindin immunostaining; scale bars, 80 μm.

cases of CS in humans (Itoh et al., 1999; Lindenbaum et al., 2001).

Discussion

Recapitulation of the XPCS phenotype in mice

Existing mouse models of CS, including CSB and CSA mice, as well as TTD mice, mimic the respective human syndromes but generally display milder disease symptoms (van der Horst et al., 1997, 2002; de Boer et al., 1998a). Possibly this is due to species-specific differences in the DNA damage response and/or time frame (see below). Consistent with this, XPCS mice displayed developmental delay and mild segmental aging features, including cachexia and testicular atrophy. XPCS mice also had a shorter mean life span—a phenotype likely at least in part related to an earlier onset of spontaneous cancers. XPCS cells revealed molecular characteristics of DNA damage repair strikingly similar to human XPD^{G602D} cells, including reduced TC-NER capacity, residual UDS activity in the absence of lesion removal, altered NER complex dynamics, reduced UV and ionizing radiation resistance, and reduced host cell reactivation of UV- and oxidative-type DNA lesions. Furthermore, XPCS mice displayed an extreme UV-induced cancer predisposition as in the human XPD^{G602D} patient. Thus, the patient-based XPD^{G602D} point mutation recapitulated in mice many elements of both the xeroderma pigmentosum and Cockayne syndrome components of the combined disorder.

It is important to note that XPCS mice did *not* display the hallmark features of TTD that set it apart from XPCS, notably brittle hair, ichthyotic skin, and anemia (data not shown), despite reduced levels of TFIIH in fibroblasts. This provides strong evidence that specific point mutations in the human *XPD* gene and its mouse counterpart result in precise pathologies in both man and rodents.

Common mechanism of segmental progeria in CS and TTD

Although a number of underlying disease mechanisms have been put forth to explain XPD disorders, we favor the notion that DNA repair of transcription-blocking lesions is a primary determinant of progeria in both XPCS and TTD. This notion initially gained traction with the genetic finding that a further reduction of DNA repair capacity in TTD and CSB mice by XPA inactivation results in accelerated progeroid features and a reduced life span of 2–3 weeks (de Boer et al., 2002; Murai et al., 2001). Here, we present further evidence in support of the hypothesis that a common disease mechanism rooted in defective DNA repair underlies the segmental progeroid features shared by TTD and XPCS.

First, we reasoned that if the basic mechanisms of progeroid disease in XPCS and TTD were different (e.g., if a TCR deficit explains CS and a gene-specific transcriptional activation insufficiency causes the premature aging in TTD), then inactivation of the exclusively NER-associated *Xpa* gene would likely result in different phenotypes in double mutant XPA|XPCS versus XPA|TTD mice. On the contrary, we found a phenotypic overlap between XPA|XPCS and XPA|TTD mice, including progressive postnatal growth failure, disproportionally large head and limbs, kyphosis, ataxia, spasticity, balance problems, cachexia, and death around 2–3 weeks of age. A similar phenotype was observed upon further inactivation of DNA repair capacity (by genetic ablation of the *Xpa* or *Xpc* gene) in mouse models of CS, including XPA|CSB, XPA|CSA, and XPC|CSB double mutant mice (Friedberg and Meira, 2004; Murai et al., 2001; van der Horst et al., 2002). A similar phenotype is also present in mice lacking the XPCS-associated *Xpg* gene (Sun et al., 2001). The overlapping phenotypes of mice with single or double homozygous mutations in various NER-associated genes are strongly suggestive of defective DNA repair, rather than defects in transcription associated with specific *Xpd* point mutations, as causative of the severe developmental phenotypes resembling the progeroid disorders CS and TTD in humans. Recent evidence of functional interactions between XPG, CSB, and stalled RNA-PII in vitro and in vivo lend further support to this conclusion (Sarker et al., 2005).

Second, we found that XPA|XPCS and XPA|TTD cells share a common deficit in the spatiotemporal organization of the GG-NER reaction at local UV-induced damage. Although GG-NER capacity does not correlate with segmental progeria, mutations affecting GG-NER components may result in similar spatiotemporal alterations of the NER reaction in response to more relevant damage types such as oxidative lesions.

Finally, spontaneously immortalized XPCS MEFs and SV40-immortalized XPCS patient-derived fibroblasts, like the corresponding TTD and CSB cells, were defective in host cell reactivation of ionizing radiation-induced DNA damage. This is important because neither human nor mouse TTD cells have been reported to be hypersensitive to acute oxidative stress (de Boer et al., 2002), confounding any interpretation of the relationship between endogenous oxidative DNA damage and NER-associated progerias. Although ionizing radiation can break the DNA sugar-phosphate backbone directly, most damage is due to oxidation of the bases by reactive oxygen species including hydroxyl radicals (Riley, 1994). These DNA lesions can be subtle base modifications and typical base excision repair substrates (e.g., 8-oxoG and thymine glycol). Some are, however, helix distorting and thus typical NER targets (e.g., 8,5′-cyclo-2′-deoxyadenosine). Combined with the known role of NER in host cell reactivation of helix-distorting oxidative lesions (Brooks et al., 2000), our data suggest that both helix-distorting and non-distorting oxidative lesions are affected in CS, XPCS, and TTD alike. Finally, the small differences in host cell reactivation of oxidative lesions between man and mouse suggest that interspecies differences in the severity of NER-associated progerias may emerge from species-specific responses to such damage.

Molecular mechanism of cancer predisposition in XPCS versus TTD

Our data suggest that reduced longevity of XPCS mice is related at least in part to enhanced spontaneous internal tumor incidence similar to that observed both in XP patients (Kraemer et al., 1987) and the XPA mouse model (H.v.S., unpublished data). Because XP can result from defects in either NER (XPA-XPG) or error-free lesion bypass (XPV), the ultimate cause of mutations underlying the skin cancer predisposition of XP patients and mice is thought to be DNA replication over unrepaired UV lesions by error-prone bypass polymerases. Although species-specific differences in cancer induction and control of repair (e.g., p53 control of XPE expression (Tang and Chu, 2002) perhaps complicate direct human-mouse comparisons, assessment among NER mutant mice is feasible. Surprisingly, we found that XPCS mice with apparent residual cellular NER activity (30% of wt UDS) appeared even more cancer prone than completely NER-defective XPA mice upon chronic exposure to UV-B. This is in sharp contrast to TTD mice, which exhibit a lower spontaneous tumor incidence than wt mice (Wijnhoven et al., 2005), are only mildly cancer prone when exposed to a high dose of UV-B (Table S1) (de Boer et al., 1999), and were cancer free when exposed to a comparably low dose (80 J/m^2/day; J.J. and H. Rebel, unpublished data).

Several observations suggest a molecular defect specific to XPCS that makes it worse than lacking NER capacity altogether. First, unlike in TTD and other NER-deficient cells, repair synthesis (as measured by UDS) failed to correlate with lesion removal specifically in *XPD*^{XPCS} and *XPD*^{XP} cells and thus does not represent actual repair. Based on its localization within locally UV-irradiated regions of the nucleus (data not shown), this phantom UDS may instead reflect DNA synthesis in the area of the damage but apart from the lesion itself, for example, on the undamaged strand opposite a lesion. Such a process would require the use of the damaged strand as a template and could lead directly to mutations.

Increased DNA incisions following UV damage, on the other hand, occurs specifically in cells from *XPD*^{XPCS} patients (Berneburg et al., 2000), though any physiological relevance has remained unclear. As shown here, a similar increase in UV-induced incisions occurs in cells from XPCS mice, indicating the consistent cross-species nature of this specific characteristic. We propose that the accelerated cancer induction in XPCS mice, compared to fully NER-deficient XPA mice, results from the well-known mutagenic and cytotoxic potential of persistent DNA strand breaks superimposed on the mutagenicity resulting from unrepaired bulky DNA adducts. The elevated genomic instability in XPCS may trigger cancer predisposition, whereas the enhanced cytotoxicity may contribute to the observed segmental progeria.

In summary, the TTD phenotype, in which aging is enhanced and spontaneous cancer reduced, supports the general notion

that aging by cell death and senescence confers protection from cancer. However, the XPCS mouse described here demonstrates that these processes are not always antagonistic, since both cancer as well as aging as different outcomes of DNA damage are enhanced at the same time. Intriguingly, these disparate phenotypes are the consequence of different point mutations in the same multifunctional gene XPD.

Experimental procedures

Derivation of mutant mice and mouse embryonic fibroblast lines

Derivation of *Xpa*$^{-/-}$ (XPA), *Csb*$^{-/-}$ (CSB), and *Xpd*$^{TTD/TTD}$ (TTD) mice and cells was described previously (de Boer et al., 1998a; de Vries et al., 1995; van der Horst et al., 1997). Details of the XPCS targeting construct will be provided upon request. Electroporation, culturing, and routine screening of 129/Ola-derived ES cells were performed as described previously (de Boer et al., 1998a). Heterozygous *Xpd*$^{XPCS\text{-}neoLoxP}$ ES cells were transiently transfected with *Cre* recombinase cDNA under puromycin selection in order to test expression from the targeted versus wt alleles by RT-PCR. Blastocyst injection and subsequent matings were performed by standard methods. Chimeras were mated with C57BL/6 mice; heterozygous progeny were intercrossed with FVB transgenic CAG-*cre* mice (Sakai and Miyazaki, 1997) yielding heterozygote *Xpd*^{XPCS} mice without the pMC-1 *neo*-LoxP cassette (Figure 1C). The presence of the G602D mutation and the absence of any other undesired mutations originating from cloning or gene targeting were verified by sequencing of cDNA from the targeted allele (BaseClear Group, The Netherlands). Standard genotyping for *Xpd*^{XPCS} mice was performed using primers F2 (5′-GGGAGCAGCTGCAGTCA-3′) and R (5′-GCAGGGCATGAAGTGGC TCC-3′) yielding a 400 bp wt product and a 529 bp product from the targeted allele following *Cre* recombination. Mice used in this study were in a 129Ola/C57BL/6/FVB mixed background unless noted differently. All experiments involving mice were judged and approved by the National Committee for Genetic Identification of Organisms and the Animal Ethical Committee and were conducted according to national and international guidelines.

Cellular DNA damage assays

UV-induced UDS and RRS as well as UV and gamma ray survival assays were performed as described previously (de Waard et al., 2003; Vermeulen et al., 1994). For UV survival, two to four experiments using at least two independent, early passage (2–5) primary MEF cell lines per genotype were performed. For gamma ray survival, two experiments using two independent spontaneously transformed cell lines per genotype were performed. Host cell reactivation was adapted from Spivak and Hanawalt (2006). Plasmid DNA (TK-firefly luciferase, CMV-renilla luciferase) was prepared by the alkaline lysis method using a Nucleobond AX kit. Damage was introduced into the CMV-renilla luciferase plasmid by treatment with UV-C (100 or 400 J/m^2), gamma rays from a cesium source (12.5–100 gy), visible light from a tungsten lamp for 0–36 min in the presence of 5 μM methylene blue, or addition of 0.5%–1.5% osmium tetraoxide at 65°C for 5 min. Methylene blue was removed by ethanol precipitation; osmium tetraoxide was removed by overnight dialysis in water. Cells (1–2 × 10^4) of log-phase cultures were seeded per well of a 96-well plate and transfected the next day with 400 ng undamaged internal control plasmid and 20 ng damaged plasmid in 5 μl Optimem I media (Gibco Invitrogen) with 0.2 μl Fugene 6 transfection reagent (Roche) according to the manufacturer's instructions. Firefly and renilla luciferase activities were measured 24 hr after transfection using the Promega Dual Luciferase Reporter Kit (E1960) according to the manufacturer's instructions. The following number of independent MEF lines was used: four wt, three XPCS, three TTD, two CSB. Patient-derived, SV40-transformed fibroblasts were as follows: two normal (CR50, VH10); two XPCS (XPCS2, XP8BR); two TTD (TTD1RO, TTD1BR); one CSB (CS1AN).

Immunohistopathology of the brain

Animals were anaesthetized (Nembutal; 50 mg/kg) and perfused with 4% paraformaldehyde in 0.1 M phosphate buffer. Sucrose-cryoprotected, gelatin-embedded brains were cut in 40 mm sagittal or coronal sections (one-half brain each). Nissl staining, acetylcholine esterase staining, and silver stainings were done according to standard procedures. Immunocytochemistry was performed in 0.1 M Tris-buffered saline using rabbit antibodies against calbindin (Sigma), dopamine (Mark), or tyroxine hydroxylase (Novus) diluted 1:1000 for 72 hr. Quantitative analyses of Purkinje cells were done with Neurolucida, NeuroExplorer, and analySIS software.

Comparative immunofluorescence analysis of the p62 subunit of TFIIH and local UV damage-related assays

Latex bead labeling and comparative immunofluorescence analysis of the p62 subunit of the TFIIH was performed as described previously (Botta et al., 2002; Vermeulen et al., 2000). Local UV damage induction and subsequent immunostaining was performed as described previously (Mone et al., 2001; Volker et al., 2001). UDS at locally irradiated domains in the nucleus was performed as described previously (Volker et al., 2001), except radioactive labeling for time point analysis was started immediately or 6 hr after UV irradiation for a period of 2 hr each. For γH2AX staining, at least 50 cells for each time point and genotype were randomly chosen. Of these, total nuclear intensity of γH2AX signal was measured using Adobe Photoshop. Allelic composition of mutant cell lines depicted in Table 2 are as follows: XP6BE = XPD$^{del36\text{-}61/R683W}$; TTD1RO = XPD$^{R658C/G713R}$; TTD1BR = p8$^{R56stop/L21P}$; TTD1BEL = XPD$^{R722W/R616P}$; XP1NE = XPD$^{G47R/L461V+del716\text{-}730}$.

Supplemental data

The Supplemental Data include one supplemental table and can be found with this article online at http://www.cancercell.org/cgi/content/full/10/2/121/DC1/.

Acknowledgments

This research was supported by the Netherlands Organization for Scientific Research (NWO) through the foundation of the Research Institute for Diseases in the Elderly, as well as grants from the NIH (1PO1 AG17242-02), NIEHS (1UO1 ES011044), EC (QRTL-1999-02002), Dutch Cancer Society (EUR 99-2004), and AICR (05-280). J.R.M. was a fellow of the Damon Runyon Cancer Research Fund (DRG 1677). We are grateful to Ruud Koppenol for photography; Brent Calder, Paul Lohman, and Yurii Aulchenko for statistical analyses; and Diederik van Deursen for plasmid reagents. J.H.J.H. is founder of DNage, a company in the field of aging and aging-related diseases.

Received: October 18, 2005
Revised: April 5, 2006
Accepted: May 17, 2006
Published: August 14, 2006

References

Batty, D.P., and Wood, R.D. (2000). Damage recognition in nucleotide excision repair of DNA. Gene *241*, 193–204.

Berneburg, M., Lowe, J.E., Nardo, T., Araujo, S., Fousteri, M.I., Green, M.H., Krutmann, J., Wood, R.D., Stefanini, M., and Lehmann, A.R. (2000). UV damage causes uncontrolled DNA breakage in cells from patients with combined features of XP-D and Cockayne syndrome. EMBO J. *19*, 1157–1166.

Bootsma, D., Kraemer, K.H., Cleaver, J.E., and Hoeijmakers, J.H. (2002). Nucleotide excision repair syndromes: Xeroderma pigmentosum, Cockayne syndrome, and trichothiodystrophy. In The Genetic Basis of Human Cancer, B. Vogelstein and K.W. Kinzler, eds. (New York: McGraw-Hill Medical Publishing Division), pp. 211–237.

Botta, E., Nardo, T., Lehmann, A.R., Egly, J.M., Pedrini, A.M., and Stefanini, M. (2002). Reduced level of the repair/transcription factor TFIIH in trichothiodystrophy. Hum. Mol. Genet. *11*, 2919–2928.

Bradsher, J., Auriol, J., Proietti de Santis, L., Iben, S., Vonesch, J.L., Grummt, I., and Egly, J.M. (2002). CSB is a component of RNA pol I transcription. Mol. Cell *10*, 819–829.

Brooks, P.J., Wise, D.S., Berry, D.A., Kosmoski, J.V., Smerdon, M.J., Somers, R.L., Mackie, H., Spoonde, A.Y., Ackerman, E.J., Coleman, K., et al. (2000). The oxidative DNA lesion 8,5′-(S)-cyclo-2′-deoxyadenosine is repaired by the nucleotide excision repair pathway and blocks gene expression in mammalian cells. J. Biol. Chem. *275*, 22355–22362.

Broughton, B.C., Steingrimsdottir, H., Weber, C.A., and Lehmann, A.R. (1994). Mutations in the xeroderma pigmentosum group D DNA repair/transcription gene in patients with trichothiodystrophy. Nat. Genet. *7*, 189–194.

Broughton, B.C., Thompson, A.F., Harcourt, S.A., Vermeulen, W., Hoeijmakers, J.H.J., Botta, E., Stefanini, M., King, M.D., Weber, C.A., Cole, J., et al. (1995). Molecular and cellular analysis of the DNA repair defect in a patient in xeroderma pigmentosum complementation group D who has the clinical features of xeroderma pigmentosum and Cockayne syndrome. Am. J. Hum. Genet. *56*, 167–174.

Broughton, B.C., Berneburg, M., Fawcett, H., Taylor, E.M., Arlett, C.F., Nardo, T., Stefanini, M., Menefee, E., Price, V.H., Queille, S., et al. (2001). Two individuals with features of both xeroderma pigmentosum and trichothiodystrophy highlight the complexity of the clinical outcomes of mutations in the XPD gene. Hum. Mol. Genet. *10*, 2539–2547.

Cleaver, J.E. (2000). Common pathways for ultraviolet skin carcinogenesis in the repair and replication defective groups of xeroderma pigmentosum. J. Dermatol. Sci. *23*, 1–11.

Coin, F., Proietti De Santis, L., Nardo, T., Zlobinskaya, O., Stefanini, M., and Egly, J.M. (2006). p8/TTD-A as a repair-specific TFIIH subunit. Mol. Cell *21*, 215–226.

Cozzarelli, N.R. (2003). Editorial expression of concern. Proc. Natl. Acad. Sci. USA *100*, 11816.

de Boer, J., de Wit, J., van Steeg, H., Berg, R.J.W., Morreau, M., Visser, P., Lehmann, A.R., Duran, M., Hoeijmakers, J.H.J., and Weeda, G. (1998a). A mouse model for the basal transcription/DNA repair syndrome trichothiodystrophy. Mol. Cell *1*, 981–990.

de Boer, J., Donker, I., de Wit, J., Hoeijmakers, J.H.J., and Weeda, G. (1998b). Disruption of the mouse xeroderma pigmentosum group D DNA repair/basal transcription gene results in preimplantation lethality. Cancer Res. *58*, 89–94.

de Boer, J., van Steeg, H., Berg, R.J.W., Garssen, J., de Wit, J., van Oostrom, C.T.M., Beems, R.B., van der Horst, G.T.J., van Kreijl, C.F., de Gruijl, F.R., et al. (1999). Mouse model for the DNA repair/basal transcription disorder trichothiodystrophy reveals cancer predisposition. Cancer Res. *59*, 3489–3494.

de Boer, J., Andressoo, J.O., de Wit, J., Huijmans, J., Beems, R.B., van Steeg, H., Weeda, G., van der Horst, G.T., van Leeuwen, W., Themmen, A.P., et al. (2002). Premature aging in mice deficient in DNA repair and transcription. Science *296*, 1276–1279.

de Laat, W.L., Jaspers, N.G.J., and Hoeijmakers, J.H.J. (1999). Molecular mechanism of nucleotide excision repair. Genes Dev. *13*, 768–785.

de Vries, A., van Oostrom, C.T.M., Hofhuis, F.M.A., Dortant, P.M., Berg, R.J.W., de Gruijl, F.R., Wester, P.W., van Kreijl, C.F., Capel, P.J.A., van Steeg, H., and Verbeek, S.J. (1995). Increased susceptibility to ultraviolet-B and carcinogens of mice lacking the DNA excision repair gene *XPA*. Nature *377*, 169–173.

de Waard, H., de Wit, J., Gorgels, T.G., van den Aardweg, G., Andressoo, J.O., Vermeij, M., van Steeg, H., Hoeijmakers, J.H., and van der Horst, G.T. (2003). Cell type-specific hypersensitivity to oxidative damage in CSB and XPA mice. DNA Repair (Amst.) *2*, 13–25.

de Waard, H., de Wit, J., Andressoo, J.O., van Oostrom, D.T.M., Riis, B., Weimann, A., Poulsen, H.E., van Steeg, H., Hoeijmakers, J.H.J., and van der Horst, G.T.J. (2004). Different effect of CSA and CSB deficiency on sensitivity to oxidative DNA damage. Mol. Cell Biol. *24*, 7941–7948.

Friedberg, E.C., and Meira, L.B. (2004). Database of mouse strains carrying targeted mutations in genes affecting biological responses to DNA damage (Version 6). DNA Repair (Amst.) *3*, 1617–1638.

Furuta, T., Ueda, T., Aune, G., Sarasin, A., Kraemer, K.H., and Pommier, Y. (2002). Transcription-coupled nucleotide excision repair as a determinant of cisplatin sensitivity of human cells. Cancer Res. *62*, 4899–4902.

Giglia-Mari, G., Coin, F., Ranish, J.A., Hoogstraten, D., Theil, A., Wijgers, N., Jaspers, N.G., Raams, A., Argentini, M., Van Der Spek, P.J., et al. (2004). A new, tenth subunit of TFIIH is responsible for the DNA repair syndrome trichothiodystrophy group A. Nat. Genet. *36*, 714–719.

Hanawalt, P.C. (2002). Subpathways of nucleotide excision repair and their regulation. Oncogene *21*, 8949–8956.

Harper, J.W., and Elledge, S.J. (1998). The role of Cdk7 in CAK function, a retro-retrospective. Genes Dev. *12*, 285–289.

Hoeijmakers, J.H. (2001). Genome maintenance mechanisms for preventing cancer. Nature *411*, 366–374.

Hoogstraten, D., Nigg, A.L., Heath, H., Mullenders, L.H., van Driel, R., Hoeijmakers, J.H., Vermeulen, W., and Houtsmuller, A.B. (2002). Rapid switching of TFIIH between RNA polymerase I and II transcription and DNA repair in vivo. Mol. Cell *10*, 1163–1174.

Itin, P.H., Sarasin, A., and Pittelkow, M.R. (2001). Trichothiodystrophy: update on the sulfur-deficient brittle hair syndromes. J. Am. Acad. Dermatol. *44*, 891–920.

Itoh, M., Hayashi, M., Shioda, K., Minagawa, M., Isa, F., Tamagawa, K., Morimatsu, Y., and Oda, M. (1999). Neurodegeneration in hereditary nucleotide repair disorders. Brain Dev. *21*, 326–333.

Keriel, A., Stary, A., Sarasin, A., Rochette-Egly, C., and Egly, J.M. (2002). XPD mutations prevent TFIIH-dependent transactivation by nuclear receptors and phosphorylation of RARα. Cell *109*, 125–135.

Kraemer, K.H., Lee, M.M., and Scotto, J. (1987). Xeroderma pigmentosum. Cutaneous, ocular, and neurologic abnormalities in 830 published cases. Arch. Dermatol. *123*, 241–250.

Lafforet, D., and Dupuy, J.M. (1978). Photosensibilite et reparation de l'ADN. Possibilite d'une parente nostologique entre xeroderma pigmentosum et syndrome de Cockayne. Arch. Fr. Pediatr. Suppl. *35*, 65–74.

Lehmann, A.R. (2003). DNA repair-deficient diseases, xeroderma pigmentosum, Cockayne syndrome and trichothiodystrophy. Biochimie *85*, 1101–1111.

Lehmann, A.R. (2005). Replication of damaged DNA by translesion synthesis in human cells. FEBS Lett. *579*, 873–876.

Lindenbaum, Y., Dickson, D., Rosenbaum, P., Kraemer, K., Robbins, I., and Rapin, I. (2001). Xeroderma pigmentosum/cockayne syndrome complex: first neuropathological study and review of eight other cases. Eur. J. Paediatr. Neurol. *5*, 225–242.

Mitchell, J.R., Hoeijmakers, J.H., and Niedernhofer, L.J. (2003). Divide and conquer: nucleotide excision repair battles cancer and ageing. Curr. Opin. Cell Biol. *15*, 232–240.

Mone, M.J., Volker, M., Nikaido, O., Mullenders, L.H., van Zeeland, A.A., Verschure, P.J., Manders, E.M., and van Driel, R. (2001). Local UV-induced DNA damage in cell nuclei results in local transcription inhibition. EMBO Rep. *2*, 1013–1017.

Murai, M., Enokido, Y., Inamura, N., Yoshino, M., Nakatsu, Y., van der Horst, G.T., Hoeijmakers, J.H., Tanaka, K., and Hatanaka, H. (2001). Early postnatal ataxia and abnormal cerebellar development in mice lacking Xeroderma pigmentosum Group A and Cockayne syndrome Group B DNA repair genes. Proc. Natl. Acad. Sci. USA *98*, 13379–13384.

Nakura, J., Ye, L., Morishima, A., Kohara, K., and Miki, T. (2000). Helicases and aging. Cell. Mol. Life Sci. *57*, 716–730.

Nance, M.A., and Berry, S.A. (1992). Cockayne syndrome: Review of 140 cases. Am. J. Med. Genet. *42*, 68–84.

O'Driscoll, M., Ruiz-Perez, V.L., Woods, C.G., Jeggo, P.A., and Goodship, J.A. (2003). A splicing mutation affecting expression of ataxia-telangiectasia and Rad3-related protein (ATR) results in Seckel syndrome. Nat. Genet. *33*, 497–501.

Rapin, I., Lindenbaum, Y., Dickson, D.W., Kraemer, K.H., and Robbins, J.H. (2000). Cockayne syndrome and xeroderma pigmentosum. Neurology *55*, 1442–1449.

Riley, P.A. (1994). Free radicals in biology: oxidative stress and the effects of ionizing radiation. Int. J. Radiat. Biol. *65*, 27–33.

Sakai, K., and Miyazaki, J. (1997). A transgenic mouse line that retains Cre recombinase activity in mature oocytes irrespective of the cre transgene transmission. Biochem. Biophys. Res. Commun. *237*, 318–324.

Sarker, A.H., Tsutakawa, S.E., Kostek, S., Ng, C., Shin, D.S., Peris, M., Campeau, E., Tainer, J.A., Nogales, E., and Cooper, P.K. (2005). Recognition of RNA polymerase II and transcription bubbles by XPG, CSB, and TFIIH: insights for transcription-coupled repair and Cockayne Syndrome. Mol. Cell *20*, 187–198.

Schaeffer, L., Roy, R., Humbert, S., Moncollin, V., Vermeulen, W., Hoeijmakers, J.H.J., Chambon, P., and Egly, J. (1993). DNA repair helicase: a component of BTF2 (TFIIH) basic transcription factor. Science *260*, 58–63.

Spivak, G., and Hanawalt, P.C. (2006). Host cell reactivation of plasmids containing oxidative DNA lesions is defective in Cockayne syndrome but normal in UV-sensitive syndrome fibroblasts. DNA Repair (Amst.) *5*, 13–22. Published online August 29, 2005. 10.1016/j.dnarep.2005.06.017.

Stefanini, M., Lagomarisini, P., Gilliani, S., Nardo, T., Botta, E., Peserico, A., Kleyer, W.J., Lehmann, A.R., and Sarasin, A. (1993). Genetic heterogeneity of the excision repair defect associated with trichothiodystrophy. Carcinogenesis *14*, 1101–1105.

Sun, X.Z., Harada, Y.N., Takahashi, S., Shiomi, N., and Shiomi, T. (2001). Purkinje cell degeneration in mice lacking the xeroderma pigmentosum group G gene. J. Neurosci. Res. *64*, 348–354.

Svejstrup, J.Q. (2003). Rescue of arrested RNA polymerase II complexes. J. Cell Sci. *116*, 447–451.

Takayama, K., Salazar, E.P., Lehmann, A., Stefanini, M., Thompson, L.H., and Weber, C.A. (1995). Defects in the DNA repair and transcription gene *ERCC2* in the cancer-prone disorder xeroderma pigmentosum group D. Cancer Res. *55*, 5656–5663.

Takayama, K., Salazar, E.P., Broughton, B.C., Lehmann, A.R., Sarasin, A., Thompson, L.H., and Weber, C.A. (1996). Defects in the DNA repair and transcription gene *ERCC2* (*XPD*) in trichothiodystrophy. Am. J. Hum. Genet. *58*, 263–270.

Tang, J., and Chu, G. (2002). Xeroderma pigmentosum complementation group E and UV-damaged DNA-binding protein. DNA Repair (Amst.) *1*, 601–616.

Taylor, E.M., Broughton, B.C., Botta, E., Stefanini, M., Sarasin, A., Jaspers, N.G., Fawcett, H., Harcourt, S.A., Arlett, C.F., and Lehmann, A.R. (1997). Xeroderma pigmentosum and trichothiodystrophy are associated with different mutations in the XPD (ERCC2) repair/transcription gene. Proc. Natl. Acad. Sci. USA *94*, 8658–8663.

Theron, T., Fousteri, M.I., Volker, M., Harries, L.W., Botta, E., Stefanini, M., Fujimoto, M., Andressoo, J.O., Mitchell, J., Jaspers, N.G., et al. (2005). Transcription-associated breaks in xeroderma pigmentosum group D cells from patients with combined features of xeroderma pigmentosum and Cockayne syndrome. Mol. Cell. Biol. *25*, 8368–8378.

van den Boom, V., Jaspers, N.G., and Vermeulen, W. (2002). When machines get stuck—obstructed RNA polymerase II: displacement, degradation or suicide. Bioessays *24*, 780–784.

van der Horst, G.T.J., van Steeg, H., Berg, R.J.W., van Gool, A., de Wit, J., Weeda, G., Morreau, H., Beems, R.B., van Kreijl, C.F., de Gruijl, F.R., et al. (1997). Defective transcription-coupled repair in Cockayne syndrome B mice is associated with skin cancer predisposition. Cell *89*, 425–435.

van der Horst, G.T., Meira, L., Gorgels, T.G., de Wit, J., Velasco-Miguel, S., Richardson, J.A., Kamp, Y., Vreeswijk, M.P., Smit, B., Bootsma, D., et al. (2002). UVB radiation-induced cancer predisposition in Cockayne syndrome group A (Csa) mutant mice. DNA Repair (Amst.) *1*, 143–157.

van Hoffen, A., Kalle, W.H., de Jong-Versteeg, A., Lehmann, A.R., van Zeeland, A.A., and Mullenders, L.H. (1999). Cells from XP-D and XP-D-CS patients exhibit equally inefficient repair of UV-induced damage in transcribed genes but different capacity to recover UV-inhibited transcription. Nucleic Acids Res. *27*, 2898–2904.

Vermeulen, W., Scott, R.J., Potger, S., Muller, H.J., Cole, J., Arlett, C.F., Kleijer, W.J., Bootsma, D., Hoeijmakers, J.H.J., and Weeda, G. (1994). Clinical heterogeneity within xeroderma pigmentosum associated with mutations in the DNA repair and transcription gene ERCC3. Am. J. Hum. Genet. *54*, 191–200.

Vermeulen, W., Bergmann, E., Auriol, J., Rademakers, S., Frit, P., Appeldoorn, E., Hoeijmakers, J.H., and Egly, J.M. (2000). Sublimiting concentration of TFIIH transcription/DNA repair factor causes TTD-A trichothiodystrophy disorder. Nat. Genet. *26*, 307–313.

Volker, M., Mone, M.J., Karmakar, P., van Hoffen, A., Schul, W., Vermeulen, W., Hoeijmakers, J.H., van Driel, R., van Zeeland, A.A., and Mullenders, L.H. (2001). Sequential assembly of the nucleotide excision repair factors in vivo. Mol. Cell *8*, 213–224.

Wang, X.W., Vermeulen, W., Coursen, J.D., Gibson, M., Lupold, S.E., Forrester, K., Xu, G., Elmore, L., Yeh, H., Hoeijmakers, J.H., and Harris, C.C. (1996). The XPB and XPD DNA helicases are components of the p53-mediated apoptosis pathway. Genes Dev. *10*, 1219–1232.

Weeda, G., Eveno, E., Donker, I., Vermeulen, W., Chevallier-Lagente, O., Taïeb, A., Stary, A., Hoeijmakers, J.H.J., Mezzina, M., and Sarasin, A. (1997). A mutation in the *XPB/ERCC3* DNA repair transcription gene, associated with trichothiodystrophy. Am. J. Hum. Genet. *60*, 320–329.

Wijnhoven, S.W., Beems, R.B., Roodbergen, M., van den Berg, J., Lohman, P.H., Diderich, K., van der Horst, G.T., Vijg, J., Hoeijmakers, J.H., and van Steeg, H. (2005). Accelerated aging pathology in ad libitum fed Xpd(TTD) mice is accompanied by features suggestive of caloric restriction. DNA Repair (Amst.) *4*, 1314–1324.